International Journal of Nanomedicine

Dovepress

open access to scientific and medical research

Open Access Full Text Article

ORIGINAL RESEARCH

NH_4HCO_3 gas-generating liposomal nanoparticle for photoacoustic imaging in breast cancer

This article was published in the following Dove Press journal:
International Journal of Nanomedicine
6 March 2017
Number of times this article has been viewed

Jizhu Xia
Gang Feng
Xiaorong Xia
Lan Hao
Zhigang Wang

Chongqing Key Laboratory of Ultrasound Molecular Imaging, Department of Ultrasound, The Second Affiliated Hospital of Chongqing Medical University, Chongqing, People's Republic of China

Abstract: In this study, we have developed a biodegradable nanomaterial for photoacoustic imaging (PAI). Its biodegradation products can be fully eliminated from a living organism. It is a gas-generating nanoparticle of liposome-encapsulating ammonium bicarbonate (NH_4HCO_3) solution, which is safe, effective, inexpensive, and free of side effects. When lasers irradiate these nanoparticles, NH_4HCO_3 decomposes to produce CO_2, which can absorb much of the light energy under laser irradiation with a specific wavelength, and then expand under heat to generate a thermal acoustic wave. An acoustic detector can detect this wave and show it as a photoacoustic signal on a display screen. The intensity of the photoacoustic signal is enhanced corresponding to an increase in time, concentration, and temperature. During in vivo testing, nanoparticles were injected into tumor-bearing nude mice through the caudal vein, and photoacoustic signals were detected from the tumor, reaching a peak in 4 h, and then gradually disappearing. There was no damage to the skin or subcutaneous tissue from laser radiation. Our developed gas-generating nanomaterial, NH_4HCO_3 nanomaterial, is feasible, effective, safe, and inexpensive. Therefore, it is a promising material to be used in clinical PAI.

Keywords: Photoacoustic tomography, CO_2, NH_4HCO_3, contrast agent, cancer

Introduction

Photoacoustic imaging (PAI) has developed rapidly in recent years. It is a non-destructive biophoton imaging method based on optical absorption differences in biological tissue and mediated by laser irradiation and ultrasound. It has the advantages of the high contrast of pure optical imagery and the high permeability of pure ultrasound; therefore, it is an important method for evaluating morphology, physiological features, metabolic functions, and pathological features of biological tissue.[1,2] PAI has promising applications in biomedical clinical diagnosis and has become a "hot topic" in recent studies. Its principle is as follows: when irradiated by a pulsed laser, a biological tissue absorbs the laser energy, causing a local temperature rise and thermoelastic expansion that generates an ultrasound signal, which can be detected by an ultrasonic detector near the tissue.[3] The photoacoustic signal is then analyzed to reconstruct an optical absorption distribution image.

However, because the biological tissue has a strong scattering effect on lasers, the light intensity and the photoacoustic signal-to-noise ratio exhibit exponential decay corresponding to the increase in tissue depth. Thus, the research direction is to develop a contrast agent to enhance the PAI effect.[4–6] At present, major materials used for PAI contrast agents include gold nanomaterials, dyes, and carbon nanomaterials.[7–12] However, the use of such materials is controversial in PAI. As a heavy metal, gold cannot be excreted by a living organism and, thus, is hazardous to health. Gold is also very

Correspondence: Lan Hao; Zhigang Wang
Chongqing Key Laboratory of Ultrasound Molecular Imaging, The Second Affiliated Hospital of Chongqing Medical University, Linjiang Road 76, Chongqing, 400010, People's Republic of China
Tel +86 23 6848 6153
Email lanhao5@163.com; wzg62942443@163.com

submit your manuscript | www.dovepress.com
Dovepress
http://dx.doi.org/10.2147/IJN.S113366

expensive. Indocyanine green is approved by the China Food and Drug Administration as a safe dye, and while a large portion of it can be eliminated, it is costly and takes a long time to be completely cleared from the body. Carbon nanotubes are not pure carbon and have a long residence time within a living organism. Only a tiny portion of them is eliminated through urine or feces, and they can cause eye discomfort, skin allergy, lung cancer, and pneumoconiosis. Because the above-mentioned contrast agents have such disadvantages as the inability to be fully eliminated by living organisms, have side effects, and are costly, they cannot be widely applied in clinical practice. Therefore, it is necessary to find a safe and inexpensive substance without side effects to serve as a contrast-enhancing material for PAI.

In our previous study, we found that not only could an NH_4HCO_3 solution emit photoacoustic signals but that all of its decomposition products are normal metabolites of the human body, can be completely eliminated from living organisms, and are nontoxic to humans. Based on the results of this study, we propose a nanoscale contrast agent made of a liposome-encapsulating NH_4HCO_3 solution that can be applied in PAI. We have evaluated its feasibility and effectiveness through in vitro qualitative and quantitative tests, explored its imaging capacity, and tested its safety and imaging effects through animal tests to lay a solid foundation for its application in PAI (Figure 1).

Materials and methods

Preparation of the nanoparticles

The thin-film hydration method plus the liposome extrusion method used in preparation was as follows: 1) At a mass ratio of 3:1:1, cholesterol-free distearoylphosphatidylcholine, distearoylphosphatidylethanolamine–polyethylene glycol 2000 (Avanti Polar Lipids, Inc., Alabaster, AL, USA), and cholesterol (Sangon Biotech Co., Ltd, Shanghai, People's Republic of China) were added to 10 mL of chloroform (Chongqing Chuandong Chemical Group Co., Ltd, Chongqing, People's Republic of China) and mixed thoroughly. 2) On a rotavapor (Shanghai Yarong Biochemical Instruments Factory, Shanghai, People's Republic of China), the above-mentioned solution was rotated at 50°C at a rotational speed of 60 rpm for ~60 min. 3) After the rotation, 5 mL of NH_4HCO_3 (Chengdu Kelong Chemical Reagent Factory, Chengdu, People's Republic of China) saturated solution was added, and the resulting solution was placed in an ultrasound cleaner (Ningbo Scientz Biotechnology Co., Ltd, Ningbo, People's Republic of China) to be shaken for a few seconds. 4) The above-mentioned solution was passed through extruder filter films (Whatman Plc, Kent, UK) with apertures of 800, 400, and 200 nm, respectively. 5) The extruded solution was dissolved in a 5% glucose solution (Chengdu Kelong Chemical Reagent Factory) for dialysis.

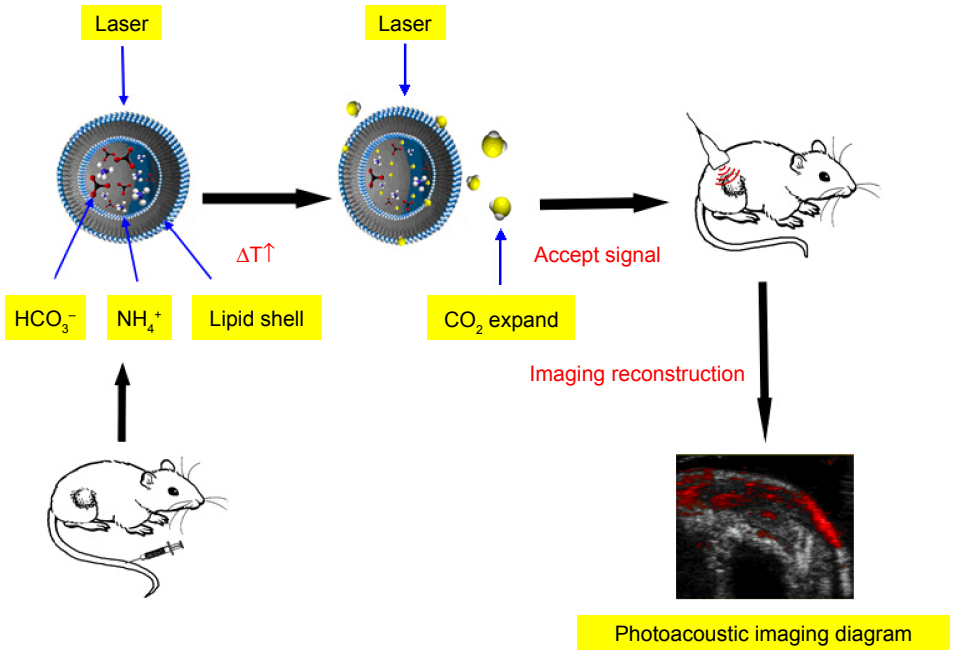

Figure 1 The generation of photoacoustic signal.
Notes: When a laser irradiates a nanoparticle, it is decomposed into CO_2, H_2O, and ammonia. CO_2 absorbs much of the light energy at a specific wavelength and expands under heat to produce a thermal acoustic wave, which can be detected by the acoustic detector and then displayed on a screen as a photoacoustic signal.
Abbreviations: HCO_3^-, bicarbonate; NH_4^+, ammonium.

Optical microscope and electron microscopy

Nanoparticle morphology and distribution were observed using a BX 54 optical microscope (Olympus Optical, Tokyo, Japan) and a S-3000N field emission scanning electron microscope (Hitachi, Tokyo, Japan); nanoparticle size and zeta potential were measured using a laser particle size analyzer (Malvern Instruments Ltd, Shanghai, People's Republic of China).

Detection of NH_4HCO_3 solution encapsulation

A $CaCl_2$ solution was added into the NH_4HCO_3 solution, double-distilled H_2O (dd H_2O)-encapsulating nanoparticles (DDHN), NH_4HCO_3 encapsulating nanoparticles (ABN), broken DDHN, and broken ABN. The changes in them were observed.

Infrared spectrometer

Absorption spectra of NH_4HCO_3 solution, CO_2, dd H_2O, and ammonia solution were determined using the Spectrum 100 infrared spectrometer (PerkinElmer, Inc., Melville, New York, NY, USA).

In vitro PAI test

The NH_4HCO_3 solution was irradiated (excitation wavelength: 680–970 nm) by the VevoLAZR PAI system (VisualSonics, Inc., Toronto, ON, Canada) to determine the optimal irradiation wavelength.

Photoacoustic signal images of NH_4HCO_3 solution, CO_2, dd H_2O, ammonia solution, ABN, and DDHN were determined using the PAI system.

The ABN and DDHN samples were irradiated using the PAI system. The changes in the two samples of photoacoustic and ultrasonic models were observed. The changes of ABN in the photoacoustic image corresponding with time, concentration, and temperature were observed.

In vivo PAI test

Animals and experimental grouping

Twelve female nude mice aged 4–6 weeks were raised and supplied by the Laboratory Animal Center of Chongqing Medical University (Chongqing, People's Republic of China). All animal experiments were carried out in accordance with the guidelines of the Ethics Committee of Chongqing Medical University, which approved the study. Twelve tumor-bearing nude mice were taken and randomly divided into two groups: 1) treatment group: 1.0 mL of ABN was injected through the caudal vein and 2) control group: 1.0 mL of water-encapsulating nanoparticles was injected through the caudal vein.

Tumor cells culture and animal model

MDA-MB-231 tumor cells are tumor cell lines subcultured by the Institute of Ultrasound Imaging of Chongqing Medical University. These cells were obtained from the Basic Medical Research Institute of Chongqing Medical University. These cells were cultured in culture flasks loaded with 10% fetal bovine serum (Gibco, Shanghai, People's Republic of China) and Dulbecco's Modified Eagle's Medium (Gibco), and incubated at 37°C with 5% CO_2 and saturated humidity. When cell concentration was ~6×10^7/mL, 0.2 mL of the cell suspension was subcutaneously injected into the nude mice on their right rear legs using a sterile syringe. In ~3 weeks, subcutaneous tumors of 8–9 mm developed.

Photoacoustic imaging

The subcutaneous tumors of tumor-bearing nude mice in each group were irradiated by the PAI system, and photoacoustic images of each group at various time points before and after injection were observed.

Observation with naked eyes

Skin integrity and damage were observed with naked eyes before and after using the PAI system.

Pathological examination

After image acquisition, the tumor-bearing nude mice were sacrificed by neck-breaking, and the tumors with adjacent skin tissues were then taken and fixed with 4% paraformaldehyde. After being paraffin embedded, sectioned, and hematoxylin and eosin (H&E) stained, the tissues were observed under an optical microscope for changes in the cell structure of skin and tumor tissue.

Statistics

The data were analyzed using SPSS 13.0 (SPSS Inc., Chicago, IL, USA). All measurement data were expressed as mean ± standard deviation (SD). The means between groups were compared using one-factor analysis of variance (ANOVA), whereas pair-wise comparisons were made using Fisher's least significant difference method. $P<0.05$ was considered statistically significant.

Results

General physical properties test

Observed under an optical microscope, nanoparticles were spherical with a regular shape and uniform size and distribution. There was no obvious aggregation with a concentration of ~2.63×10^{10}/mL counted manually (Figure 2).

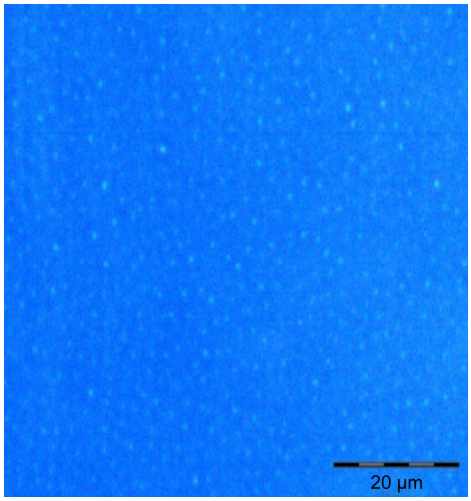

Figure 2 Optical image of nanoparticles (1,000-fold).
Note: Nanoparticles were spherical with a regular shape and uniform size and distribution.

Observation of a single nanoparticle under a transmission electron microscope (TEM) showed a two-layer phospholipid membrane on the outer compartment of the nanoparticle and NH_4HCO_3 solution filling the core (Figure 3).

Measured by a laser particle size analyzer, the mean particle size of nanoparticles was 230.9±54.58 nm, with uniform distribution and dispersion. The zeta potential was –22.8±5.75 mV.

Detection of NH_4HCO_3 solution encapsulation

The NH_4HCO_3 solution appeared to have a large amount of white precipitate. The broken ABN sample changed from clear to white. There was no other color change observed before or after $CaCl_2$ solution was added into DDHN, broken DDHN, and ABN (Figure 4).

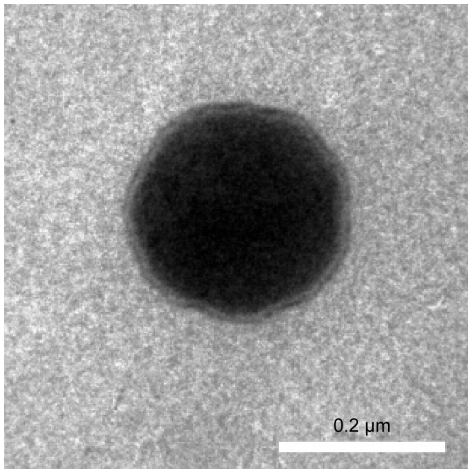

Figure 3 Transmission electron microscope image of nanoparticles.
Note: The image shows a two-layer phospholipid membrane on the outer compartment of the nanoparticle and ammonium bicarbonate solution filling the core.

Study on PAI mechanism by the ABN

The spectra of the NH_4HCO_3 solution, the ammonia solution, dd H_2O, and CO_2 were acquired using the infrared spectrometer. The results showed that absorption peak of the ammonium bicarbonate solution was at ~1,300 nm, ammonia solution at ~1,100 nm, dd H_2O at ~720 nm, and CO_2 at ~700 nm (Figure 5).

The optimal laser excitation wavelength

The NH_4HCO_3 solution was irradiated with the PAI system at laser excitation wavelengths ranging from 680 to 970 nm; the results showed that the photoacoustic signal intensity was optimal at an excitation wavelength of ~700 nm (Figure 6).

Gel models loaded with the NH_4HCO_3 solution, dd H_2O, and ammonia solution were irradiated with the PAI system. The results showed that the NH_4HCO_3 solution emitted a photoacoustic signal, whereas the dd H_2O and ammonia solution emitted no photoacoustic signal (Figure 7).

There was no photoacoustic signal recorded before the infusion of pure CO_2 into the sealing device, whereas there was a photoacoustic signal recorded after the infusion of pure CO_2 (Figure 8).

We could see that the ABN had a photoacoustic signal and ultrasonic echo enhancement, but the DDHN did not (Figure 9).

In vitro PAI experiment

Changes in the photoacoustic signal of ABN and NH_4HCO_3 solution corresponding with time

ABN samples were irradiated with the PAI system, and the results showed that the photoacoustic signal intensity gradually increased with time to reach a peak and then gradually decreased with time. The NH_4HCO_3 solution reached a peak in a short period of time and decreased soon after (Figure 10).

Changes in the photoacoustic signal of ABN at different concentrations

For serial 2-fold diluted nanoparticle samples irradiated with the PAI system, the photoacoustic signal intensity serially decreased with decreasing concentration (Figures 11 and 12).

Changes in the photoacoustic signal of ABN at different temperatures

The samples irradiated with the PAI system at different ambient temperatures (25°C, 37°C, and 42°C) showed the

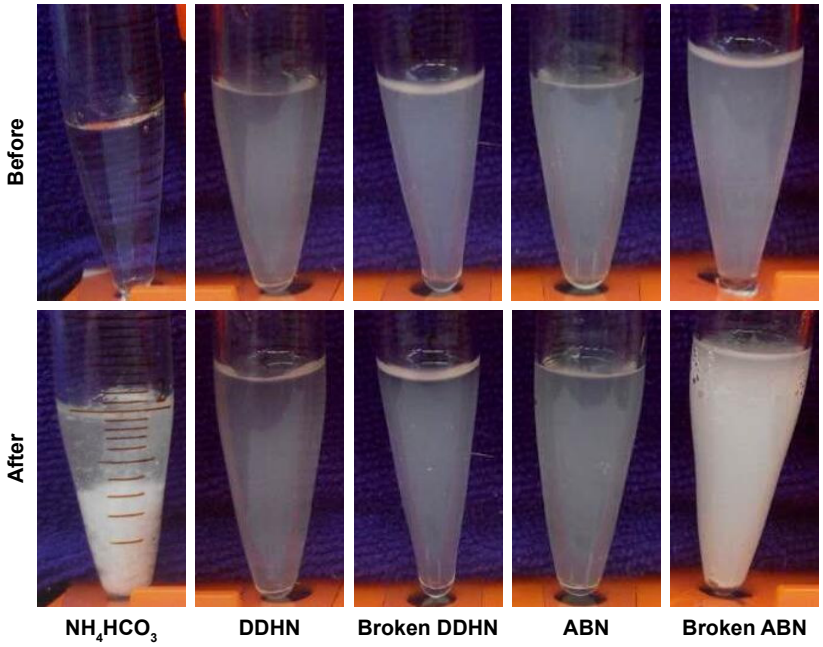

Figure 4 Change of $CaCl_2$ added into the NH_4HCO_3 solution, DDHN, broken DDHN, ABN, and broken ABN.
Abbreviations: ABN, ammonium bicarbonate-encapsulating nanoparticles; DDHN, double-distilled H_2O-encapsulating nanoparticles.

photoacoustic signal intensities of 0.56±0.11, 0.9±0.21, and 0.91±0.15, respectively. Compared to the samples at 37°C and 42°C, the sample at 25°C had the weakest photoacoustic signal intensity. There was no statistical difference found in the photoacoustic signal intensities between the samples at 42°C and 37°C ($P>0.05$; Figures 13 and 14).

In vivo PAI experiment

Intratumoral PAI

Irradiating subcutaneous tumors with the PAI system showed that the treatment group recorded no photoacoustic signal before injection, and only a slight photoacoustic signal was detected 30 min after injection. The signal gradually

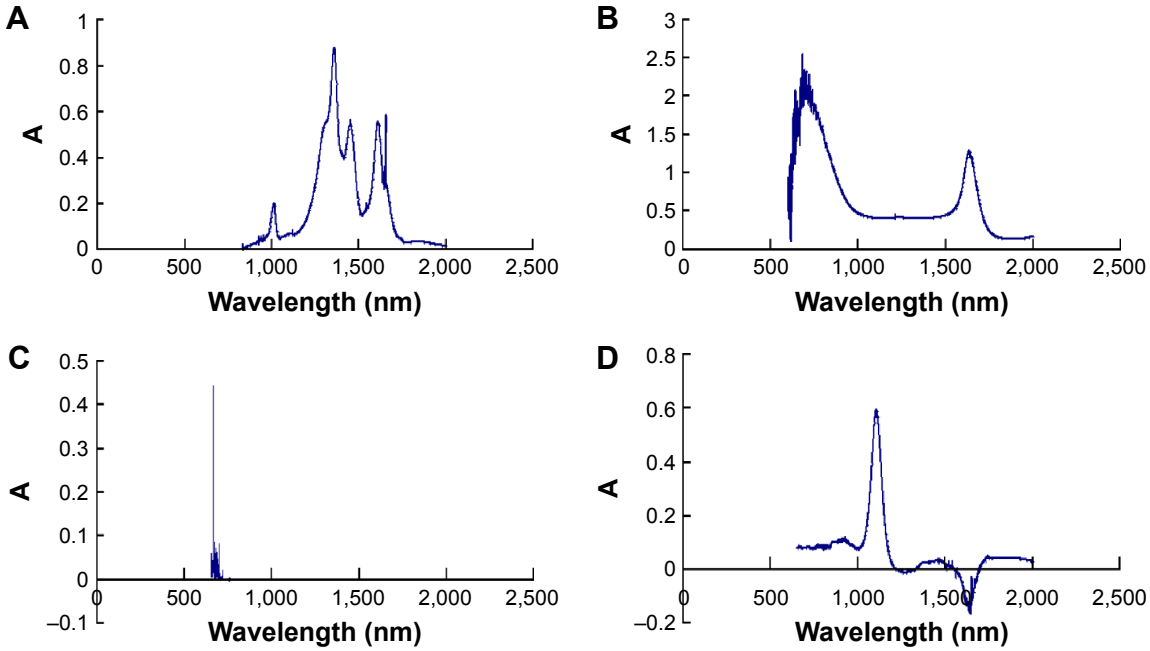

Figure 5 Infrared absorption spectra of various substances.
Notes: The absorption peaks of the NH_4HCO_3 solution were at ~1,300 nm, of the ammonia solution at ~1,100 nm, of dd H_2O at ~720 nm, and of CO_2 at ~700 nm. (**A**) NH_4HCO_3 solution. (**B**) dd H_2O. (**C**) CO_2. (**D**) Ammonia solution. 'A' means absorption peak.
Abbreviations: dd H_2O, double-distilled H_2O; NH_4HCO_3, ammonium bicarbonate.

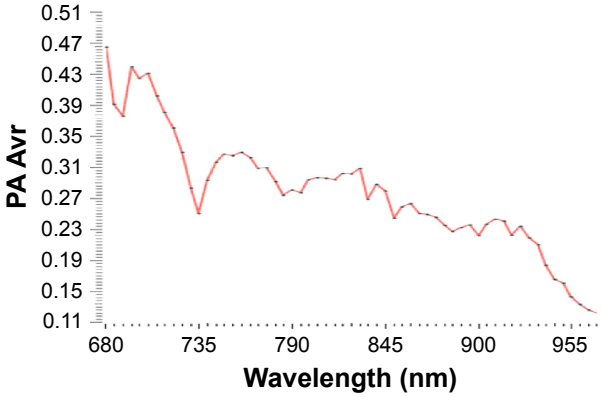

Figure 6 Photoacoustic signal images of NH_4HCO_3 solution at different near-IR wavelengths.
Abbreviations: IR, infrared; NH_4HCO_3, ammonium bicarbonate.

increased 1 h after injection; the increased signal intensity, which reached its peak 4 h after injection, gradually decreased and then completely disappeared 24 h after injection. No photoacoustic signal was observed in the control group before or after injection (Figures 15 and 16).

Tumors were observed with naked eyes

After laser irradiation, the skin had no redness, but was not swollen, and had injury (Figure 17).

Pathological examination

After H&E staining, tissues from skin and subcutaneous tumors were observed under an optical microscope. There had been no marked difference observed in the cell morphology, cell nucleus, and cytomembrane. There was no obvious necrosis and the structure of tumor tissue was not damaged (Figure 18).

Discussion

NH_4HCO_3 is a weak alkaline compound with a molecular weight of 79.06. It is a white powder and a food additive that was approved by the Food and Drug Administration of the United States in 1985. It is safe, hazard-free, and inexpensive.

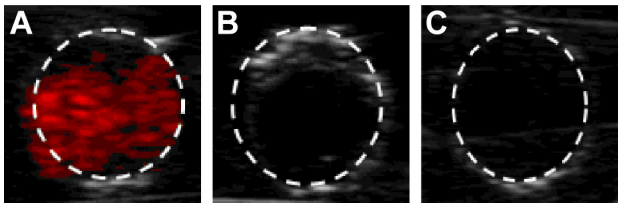

Figure 7 Photoacoustic signal images of various substances.
Notes: The NH_4HCO_3 solution has a photoacoustic signal, the ammonia solution and dd H_2O have no photoacoustic signal. (**A**) NH_4HCO_3 solution. (**B**) Ammonia solution. (**C**) dd H_2O. The positive result is represented within the dotted lines.
Abbreviations: dd H_2O, double-distilled H_2O; NH_4HCO_3, ammonium bicarbonate.

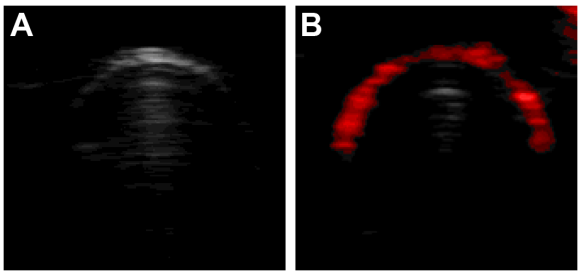

Figure 8 Photoacoustic signal images of pure CO_2.
Notes: There was no photoacoustic signal before the infusion of pure CO_2. There was photoacoustic signal after the infusion of pure CO_2. (**A**) Photoacoustic images before the infusion of pure CO_2. (**B**) Photoacoustic images after the infusion of pure CO_2.

NH_4HCO_3 decomposes into water, ammonia, and carbon dioxide without leaving any residue; all the decomposition products are normal metabolites of the human body, which are completely eliminated through the respiratory, digestive, and urinary systems.

Our preliminary research showed that a saturated NH_4HCO_3 solution could emit photoacoustic signals. To investigate the cause of the photoacoustic signals, we analyzed the NH_4HCO_3 solution, the ammonia solution, dd H_2O, and CO_2 using an infrared spectrometer. The results showed that the absorption peak of CO_2 is at ~700 nm and that of dd H_2O is at ~720 nm. In this study, the laser excitation wavelength ranged between 680 and 970 nm, suggesting that dd H_2O and CO_2 could absorb light energy within this range. We then tested all the samples using the PAI system. First, we needed to confirm the excitation wavelength. When the NH_4HCO_3 solution was irradiated by the laser at a wavelength of 680–970 nm from the PAI system, it was

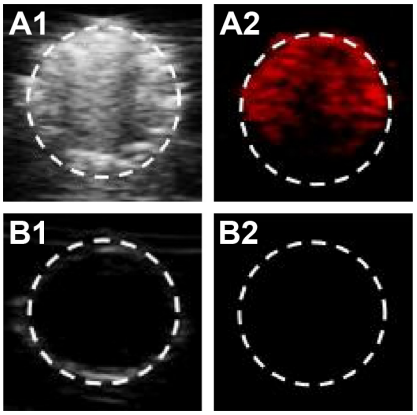

Figure 9 Ultrasonic/photoacoustic model imaging of two nanoparticles.
Notes: ABN had an ultrasonic/photoacoustic signal. DDHN had no ultrasonic/photoacoustic signal. (**A1**, **A2**) Ultrasonic/photoacoustic imaging of ABN. (**B1**, **B2**) Ultrasonic/photoacoustic imaging of DDHN. The positive result is represented within the dotted lines.
Abbreviations: ABN, ammonium bicarbonate-encapsulating nanoparticles; DDHN, double-distilled H_2O-encapsulating nanoparticles.

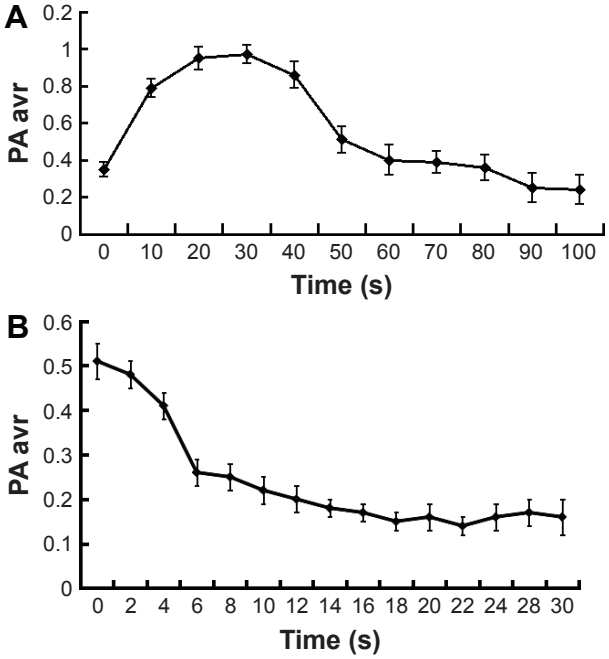

Figure 10 Time versus photoacoustic signal intensity.
Notes: Photoacoustic signal intensity of ABN gradually increased with time to reach a peak, and then gradually decreased with time. The NH_4HCO_3 solution reached a peak in a short period of time, and decreased soon after. (**A**) ABN. (**B**) NH_4HCO_3 solution.
Abbreviations: ABN, ammonium bicarbonate-encapsulating nanoparticles; NH_4HCO_3, ammonium bicarbonate.

found that the optimal photoacoustic signal was at the 700 nm wavelength. This wavelength is consistent with that of the strongest absorption peak of CO_2 detected by the infrared spectrometer, indicating that the excitation wavelength is the optimal wavelength of CO_2, and that the photoacoustic signal arises from CO_2. Therefore, 700 nm was selected as

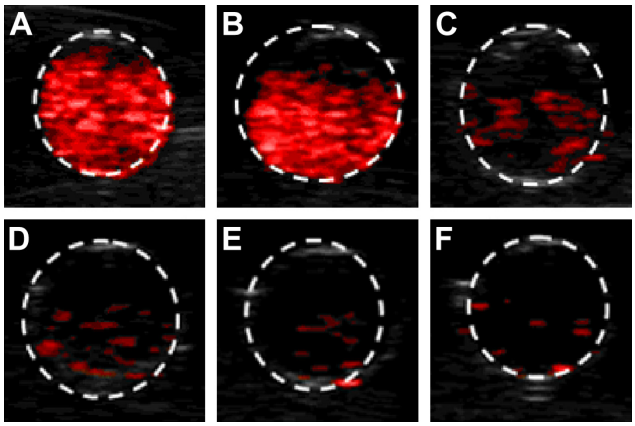

Figure 11 Concentration of ammonium bicarbonate-encapsulating nanoparticles versus photoacoustic signal images.
Notes: Photoacoustic signal intensity serially decreased with decreasing concentration. (**A**) The original concentration. (**B**) The 2-fold diluted concentration. (**C**) The 4-fold diluted concentration. (**D**) The 8-fold diluted concentration. (**E**) The 16-fold diluted concentration. (**F**) The 32-fold diluted concentration. The positive result is represented within the dotted lines.

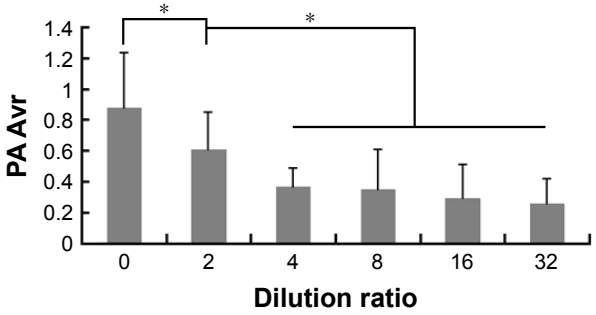

Figure 12 Concentration of ammonium bicarbonate-encapsulating nanoparticles versus photoacoustic signal intensity.
Note: *Statistical significance.

the excitation wavelength in this study. Our results showed that the NH_4HCO_3 solution and CO_2 produced photoacoustic signals, whereas the other samples did not. Therefore, we propose the following explanation: the NH_4HCO_3 solution is irradiated by a laser, and the water absorbs the light energy and converts it into heat energy, which causes NH_4HCO_3 to decompose into CO_2, ammonia, and water. Ammonia is extremely highly soluble in water, whereas CO_2 has poor water solubility, with most of it remaining in gas form. After being irradiated by a laser at a specific wavelength, the CO_2 absorbs much of the light energy at a specific wavelength and expands under heat to produce a thermal acoustic wave, which can be detected by the acoustic detector and then displayed on a screen as a photoacoustic signal.

In our previous study, we also found that the photoacoustic signal only lasted for a short time when the NH_4HCO_3 solution was irradiated by the PAI system. As we know, NH_4HCO_3 exists in the solution as HCO_3^- and NH_4^+. HCO_3^- tends to be neutralized by the acidic buffer pair in the blood, and NH_4^+ tends to transform into urea in the liver and is excreted in the urine. Therefore, it is very difficult to achieve PAI at the target area. It is necessary to encapsulate NH_4HCO_3 with a shell membrane to prevent it from being neutralized by the buffer pair in the blood,

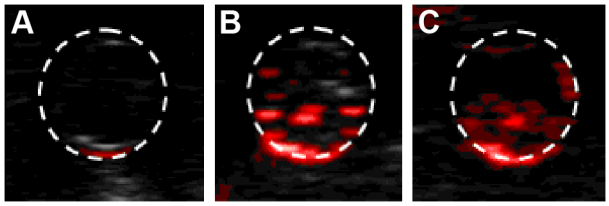

Figure 13 Temperature of ammonium bicarbonate-encapsulating nanoparticles versus photoacoustic signal image.
Notes: There was no photoacoustic signal at 25°C. But there was a photoacoustic signal at 37°C and 42°C. (**A**) 25°C. (**B**) 37°C. (**C**) 42°C. The positive result is represented within the dotted lines.

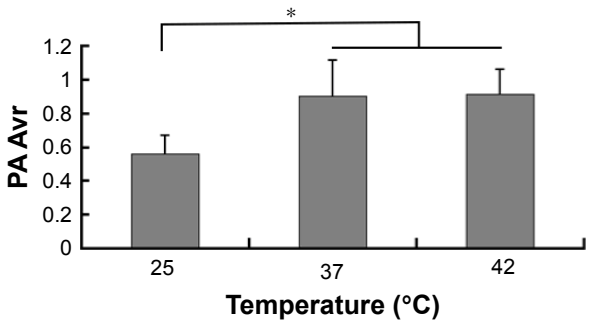

Figure 14 Temperature of ammonium bicarbonate-encapsulating nanoparticles versus photoacoustic signal intensity.
Notes: There is no significant difference between 37°C and 42°C. But there is a significant difference between 25°C and 37°C and/or 42°C. *Statistical significance.

to reduce its transformation in the liver, and to prolong the time of the photoacoustic signal. As an enveloping membrane, a liposome has characteristics such as good biocompatibility, stability, elasticity, and thinness and has been successfully applied in clinical practice. Therefore, we employed a thin-film hydration method plus an extrusion method to encapsulate the saturated NH_4HCO_3 solution in a spherical liposomal vesicle and prepared nanoparticles of phospholipid membrane encapsulating NH_4HCO_3. After testing with an optical microscope, an electron microscope, a laser particle size analyzer, and a zeta potential analyzer, results showed that the nanoparticles in the sample appeared to be spherical with a regular shape, a relatively uniform size of ~230 nm, and with a potential of ~−23 mV. The nanoparticles are smaller than the intercellular space of newly formed tumor endothelial cells, which allows the nanoparticles to cross the intercellular space and move into the tumor tissues.[13]

To verify that the NH_4HCO_3 solution was packaged in a liposome, we used a $CaCl_2$ solution. From the changes in each sample, we could see that the membranes of ABN

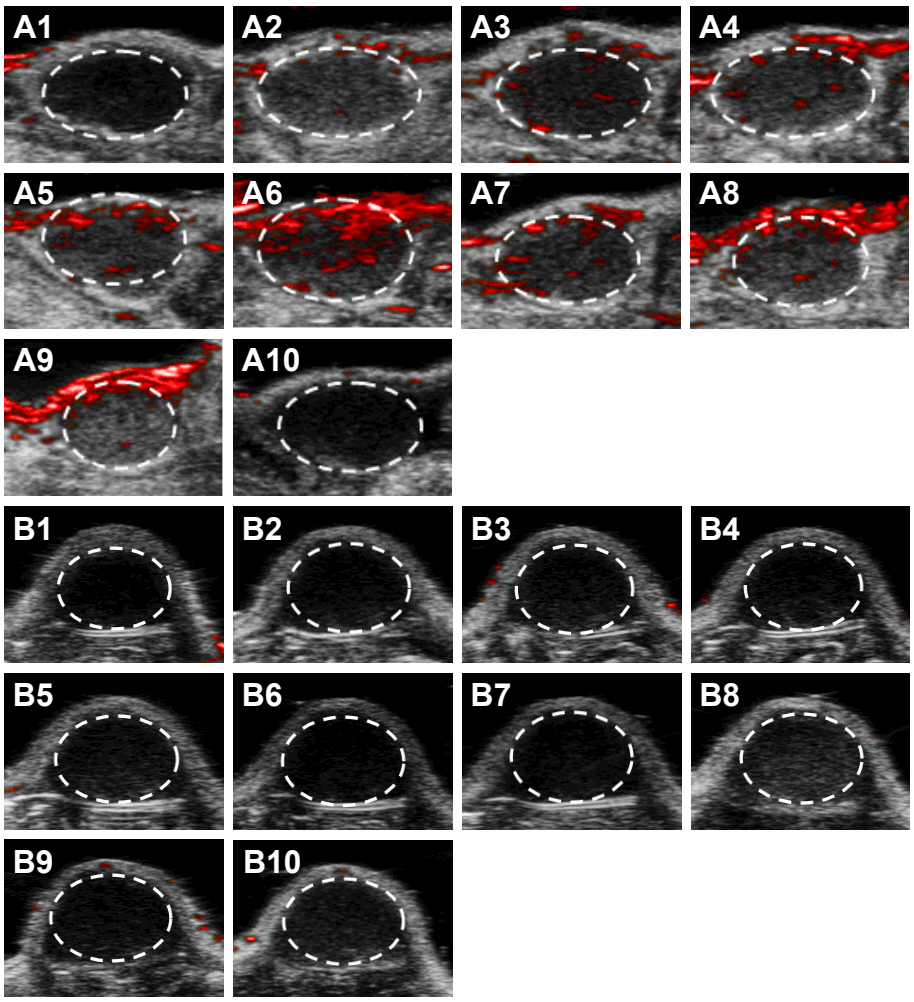

Figure 15 Photoacoustic images of subcutaneous tumor in each group.
Notes: Treatment group recorded photoacoustic signal with time. Control group recorded no photoacoustic signal with time. (**A1**–**A10**) Treatment group (**A1**: before injection, **A2**–**A10**: 30 min, 1, 2, 3, 4, 5, 6, 12, and 24 h after injection, respectively). (**B1**–**B10**) Control group (**B1**: before injection, **B2**–**B10**: 30 min, 1, 2, 3, 4, 5, 6, 12, and 24 h after injection, respectively). The positive result is represented within the dotted lines.

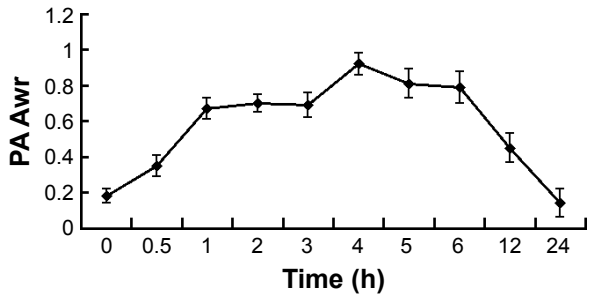

Figure 16 Time of irradiating subcutaneous tumors for the treatment group versus photoacoustic signal intensity.
Note: The photoacoustic signal value increases gradually with time and then lowers gradually.

were broken and the NH_4HCO_3 solution overflowed. When the $CaCl_2$ solution was mixed into the NH_4HCO_3 solution, the NH_4HCO_3 solution changed from clear to muddy (white precipitation/white precipitate). By contrast, the membrane of ABN had no sign of destruction, the NH_4HCO_3 solution was still enveloped in the liposome, and the $CaCl_2$ solution did not react with the NH_4HCO_3 solution. There was no change in color (from clear to muddy) indicating that DDHN and broken DDHN had not enveloped the NH_4HCO_3 solution. From the above-described phenomenon, we could deduce that the NH_4HCO_3 solution was enveloped in a liposome.

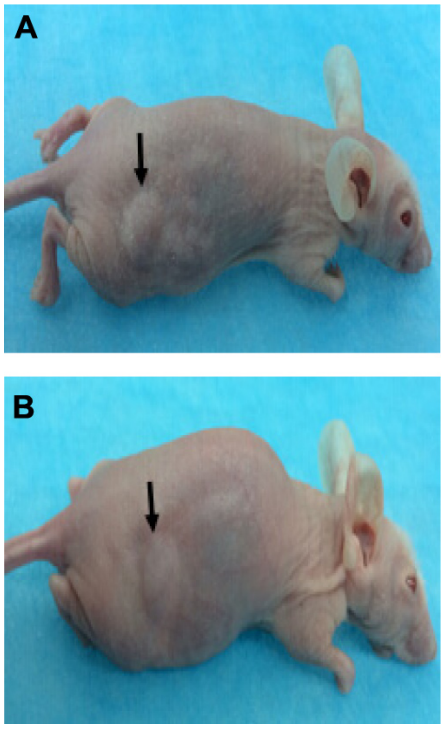

Figure 17 Observation of subcutaneous tumors with naked eyes.
Notes: After laser irradiation, the skin had no redness, but was swollen, and had injury. (**A**) Before laser irradiation. (**B**) After laser irradiation. Arrows point to the subcutaneous tumor.

At the same time, we tested ABN and DDHN using the PAI system. The photoacoustic model showed that ABN had a photoacoustic signal, while the DDHN did not. And the ultrasonic model showed an enhanced echo of ABN, while the DDHN did not. Several studies have reported the enhanced echo of ABN caused by CO_2.[14–16] Our study also found that ABN had echo and photoacoustic signals, which further demonstrated that photoacoustic signals are caused by CO_2.

We then investigated the changes in the photoacoustic signal of the ABN and NH_4HCO_3 solutions with regard to time duration. Our results showed that the photoacoustic signal intensity of ABN gradually increased, and then slowly decreased as the irradiation time was progressively lengthened. The photoacoustic signal of the NH_4HCO_3 solution quickly reached a peak value and decreased soon after. This phenomenon might be related to the rate and amount of CO_2 generated by NH_4HCO_3. After being irradiated by a laser, the ABN generate CO_2, which is inside the liposomal vesicles. Owing to its small molecular weight, CO_2 continuously diffuses across the thin phospholipid membranes out of the spherical vesicles, and then expands under laser irradiation to emit photoacoustic signals that can be detected by the detector. When the generated CO_2 decreases, the photoacoustic signal slowly decreases accordingly. The likely the cause of the change in the photoacoustic signals of ABN over time is the fact that under heat, NH_4HCO_3 decomposes into CO_2, which is inside the liposomal vesicles, and continuously diffuses out of the vesicles and gradually decreases. Conversely, there were no membranes to encapsulate the NH_4HCO_3 solution, which was not enveloped in liposome. The decomposed CO_2 was entirely released quickly, producing a photoacoustic signal in a short period of time.

In addition, we investigated the changes in the photoacoustic signals of ABN at different concentrations of ABN (~2.63×10^{10}/mL) in vitro. For serial 2-fold diluted ABN samples irradiated with the PAI system, we found that the photoacoustic signal intensity decreased corresponding with a decreased concentration. When the concentrations were higher, the photoacoustic signal was stronger; and when the concentrations were lower, the photoacoustic signal was weaker. The above-described phenomenon is presumably related to the ABN volume. As the ABN volume decreased, the generated CO_2 and the photoacoustic signals also decreased. Furthermore, we investigated the changes in the photoacoustic signals of ABN at different temperatures (25°C, 37°C, and 42°C) in vitro. At ambient temperature

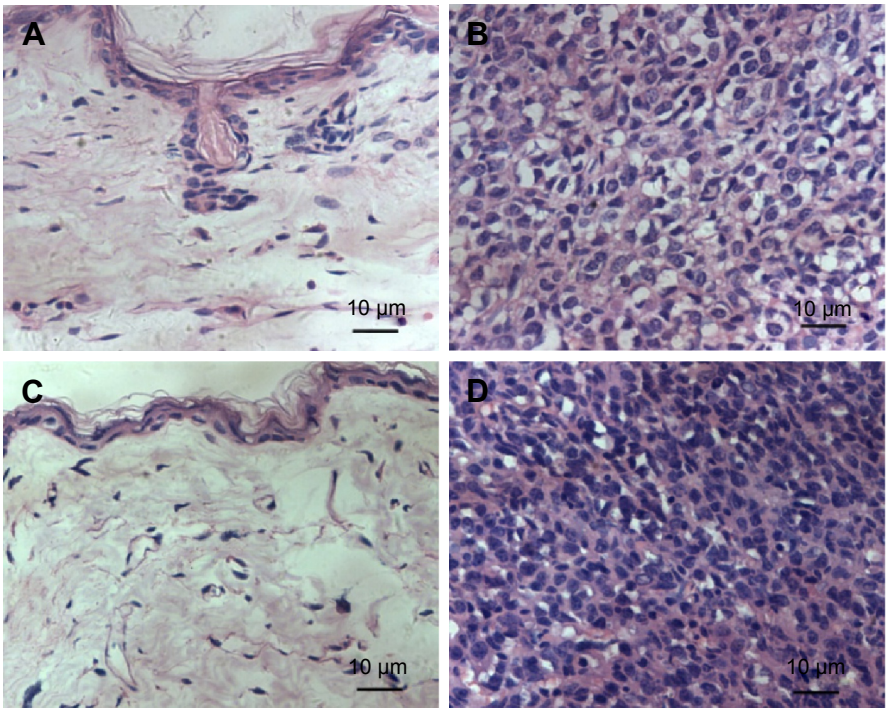

Figure 18 Hematoxylin and eosin-stained subcutaneous tumor tissue. There was no marked difference in the cell morphology, cell nucleus, and cytomembrane. There was no obvious necrosis, and the structure of tumor tissue was not damaged.
Notes: (**A**) Laser-irradiated skin (400-fold). (**B**) Laser-irradiated tumor (400-fold). (**C**) Laser non-irradiated skin (400-fold). (**D**) Laser non-irradiated tumor (400-fold).

(25°C), photoacoustic signal intensity of the sample was the weakest, and at 37°C, it increased. At 42°C, the photoacoustic signal intensity of the sample was not significantly different from that at 37°C, suggesting that the generation of photoacoustic signals of the ABN is related to temperature. Most likely, NH_4HCO_3 tends to decompose at elevated temperatures. The more CO_2 generated, the greater and stronger the photoacoustic signal. The temperature of the human body is 37°C, and at this temperature, there were stronger photoacoustic signals recorded, which provided theoretical basis for further tests in vivo.

During in vivo testing, 1.0 mL of ABN was injected through the caudal vein into tumor-bearing mice. Photoacoustic signals from subcutaneous tumors began to appear after 30 min and gradually increased to reach their peak after 4 h, when the scope of the photoacoustic signals was the largest. The signals then gradually decreased and completely disappeared after 24 h. These results indicate that the intravenously injected ABN could enter the local tumor and emit photoacoustic signals. The skin of the tumor area showed no damage and appeared intact when observed by the naked eye. Pathological examination also showed that the structure of the skin and tissue cells around the tumor were intact without obvious damage, indicating that laser energy was safe and did not cause damage to the skin or subcutaneous tumor tissues and cells.

This study used a PAI system to conduct feasible, effective, and safe in vitro and in vivo tests of liposome-derived, gas-generating nanoparticles, and elaborated the mechanism of generating photoacoustic signals. However, the following limitations remain in this study: 1) The stability of ABN is poor, 2) the potential toxicity of ABN to normal tissue or cells was not studied, and 3) there was no direct method to prove that NH_4HCO_3 was wrapped in liposomes. Therefore, further experimental studies need to be conducted to improve the stability and safety of ABN and to verify NH_4HCO_3 that was wrapped in liposomes.

Conclusion

In summary, we have succeeded in preparing a biodegradable material (NH_4HCO_3 nanoparticles) as a PAI contrast agent whose metabolic products can be completely eliminated from a living organism. The mechanism involved may be CO_2, which swells under specific optical laser wavelengths. This material, which is a liposome-encapsulating NH_4HCO_3 solution, is feasible, effective, safe, and inexpensive. Therefore, NH_4HCO_3 nanoparticles are a promising material to be used in clinical PAI for breast or superficial cancers.

Acknowledgments

We acknowledge the financial support from the National Natural Science Foundation of China (Nos 81501481 and 81401503), Projects of Sichuan Provincial Science and Technology Department (No 2015SZ0116), and Chongqing Municipal Postdoctoral Science Foundation (No Xm2014124).

Disclosure

The authors report no conflicts of interest in this work.

References

1. Yao J, Xia J, Wang LV. Multiscale functional and molecular photoacoustic tomography. *Ultrason Imaging*. 2016;38(1):44–62.
2. Kim J, Lee D, Jung U, Kim C. Photoacoustic imaging platforms for multimodal imaging. *Ultrasonography.* 2015;34(2):88–97.
3. Wang LV, Hu S. Photoacoustic tomography: in vivo imaging from organelles to organs. *Science.* 2012;335(6075):1458–1462.
4. Gutrath BS, Beckmann MF, Buchkruner A, et al. Size-dependent multispectral photoacoustic response of solid and hollow gold nanoparticles. *Nanotechnology.* 2012;23(22):225707.
5. Ku G, Zhou M, Song S, Huang Q, Hazle J, Li C. Copper sulfide nanoparticles as a new class of photoacoustic contrast agent for deep tissue imaging at 1064 nm. *ACS Nano.* 2012;6(8):7489–7496.
6. Chao W, Ma XX, Ye SQ, et al. Protamine functionalized single-walled carbon nanotubes for stem cell labeling and in vivo Raman/magnetic resonance/photoacoustic triple-modal imaging. *Adv Funct Mater.* 2012; 22(11):2363–2375.
7. Song KH, Kim CH, Cobley CM, Xia Y, Wang LV. Near-infrared gold nanocages as a new class of traces for photoacoustic sentinel lymph node mapping on a rat mode. *Nano Lett.* 2009;9(1):183–188.
8. Zhang Q, Iwakuma N, Sharma P, et al. Gold nanoparticles as a contrast agent for in vivo tumor imaging with photoacoustic tomography. *Nanotechnology.* 2009;20(39):395102.
9. Agarwal A, Huang SW, O'Donnell M, Day CK, Day M, Kotov N. Targeted gold nanorod contrast agent for prostate cancer diction by photoacoustic imaging. *J Applied Physics.* 2007;102(9):064701.
10. Lu W, Huang Q, Ku G, et al. Photoacoustic imaging of living mouse brain vasculature using hollow gold nanospheres. *Biomaterials.* 2010;31(9): 2617–2626.
11. Kanazaki K, Sano K, Makino A, et al. Development of human serum albumin conjugated with near-infrared dye for photoacoustic tumor imaging. *J Biomed Opt*. 2014;19(9):96002.
12. Gong H, Peng R, Liu Z. Carbon nanotubes for biomedical imaging: the recent advances. *Adv Drug Deliv Rev*. 2013;65(15):1951–1963.
13. Maeda H, Nakamura H, Fang J. The EPR effect for macromolecular drug delivery to solid tumors: improvement of tumor uptake, lowering of systemic toxicity, and distinct tumor imaging in vivo. *Adv Drug Deliv Rev*. 2013;65(1):71–79.
14. Minfan C, Kojie C, Hsingfa L, et al. A liposmal system capable of genrating CO_2 bubbles to induce transient cavitation, lysosomal rupturing, and cell necrosis. *Angew Chem Int Ed Engl.* 2012;51(40): 10089–10093.
15. Eunah K, Hyunsu M, Jaeyoung L, et al. Nanobubbles from gas-generationg polymeric nanoparticles: ultrasound imaging of living subjects. *Angew Chem Int Ed Engl.* 2010;49(3):524–528.
16. Chen KJ, Liang HF, Chen HL, et al. A thermoresoponsive bubble-generating liposomal system for triggering localized extracellular drug delivery. *ACS Nano*. 2013;7(1):438–446.